Soft-Probe-Scanning Electrochemical Microscopy reveals electrochemical surface reactivity of E. coli biofilms

Soft-probe-scanning electrochemical microscopy reveals electrochemical surface reactivity of *E. coli* biofilms

Sorour Darvishi [a], Horst Pick [b], Emad Oveisi [c], Hubert H. Girault [a,*], Andreas Lesch [d,*]

[a] *Laboratory of Physical and Analytical Electrochemistry, Ecole Polytechnique Fédérale de Lausanne (EPFL) Valais Wallis, Rue de l'Industrie 17, 1950, Sion, Switzerland* [b] *Environmental Engineering Institute, GR-LUD, Ecole Polytechnique Fédérale de Lausanne (EPFL), School of Architecture, Civil and Environmental Engineering, EPFL Station 2, 1015, Lausanne, Switzerland*

[c] *Interdisciplinary Center for Electron Microscopy, École Polytechnique Fédérale de Lausanne (EPFL), CH-1015, Lausanne, Switzerland*

[d] *Department of Industrial Chemistry "Toso Montanari", University of Bologna, Viale del Risorgimento 4, 40136, Bologna, Italy*

Article Info:

Keywords:
E. coli biofilm
Bioimaging
Scanning electrochemical microscopy
Soft microelectrodes
Approach curves

Abstract:

Investigating and understanding dynamic biofilm growth mechanisms is challenging, often because state-of-the- art optical characterization tools provide limited information. Micrometric electrochemical imaging of *Escher-ichia coli* biofilms using Soft-Probe-Scanning Electrochemical Microscopy (Soft-Probe-SECM) is herein presented as a complementary technique. A soft microelectrode is scanned over biofilms in a gentle contact mode, which is essential to provide a constant working distance. The on-film reduction of an electro-active compound, here the oxidized form of ferrocene methanol, is used to create *in situ* biofilm metabolic activity maps by applying the feedback mode of SECM. SECM approach curves of identically grown biofilms suggest that the SECM-baseddetection of metabolic activity is surface-confined. The analysis could therefore be carried out on entire bio-films as well as on tape-stripped biofilm surface layers. The method is further capable of distinguishing between biofilms containing *E. coli* cells either with or without ampicillin-resistance. Finally, the SECM detection of the degradation of an *E. coli* biofilm in the presence of different gentamicin concentrations is presented.

1. Introduction

About 65 % of all bacterial infections and 80 % of chronic infections in the human body are linked to bacterial biofilm formation [1]. Apart from certain parts of the human body (*e.g.* chronic wounds and urinary tract) [2], biofilms play also an important role on environmental surfaces (*e.g.*, rocks or plants) and medical implants (*e.g.* suture, catheters, and dental implants). Biofilms are of serious universal concern due to their increased tolerance to antibiotics. They can be up to 1000 times more resistant to antibiotics compared to free-floating bacterial cells [3]. The formation as well as the composition of biofilms are complex, which complicates analysis and data interpretation. Biofilms contain bacterial cells and an extracellular matrix. In addition, concentration gradients of nutrients, signalling compounds, and bacterial waste products result from the metabolic activities of the cells and their transport along diffusional channels inside the biofilms. Bacterial cells directly affect but also respond immediately to their microenvironment leading to structural, chemical, and biological heterogeneity within biofilms [4]. Moreover, during the growth and maturation of biofilms, sufficient nutrient supply will inevitably get constrained for the bacteria deeply trapped inside the biofilms [4]. As a consequence of the lack of nutrients, bacteria can escape from the sessile status of the biofilm and spread to new locations. Although much progress has been made in recent years, still little is known about biofilm growth and the development of its defence mechanisms [5]. This is often linked to the limited information that can be obtained by using state-of-the-art analytical methods, which include, for instance, the Tissue Culture Plate method [6], Tube adherence method [7], Congo Red Agar method [8], bioluminescent assays [9], and fluorescent microscopic examination [10]. Scanning electron microscopy is applied to visualize the morphology of biofilms, but it cannot measure the viability of bacteria. Fluorescence microscopy relies on dyes and might require bacterial cell fixation [11]. High-resolution techniques, such as electron and fluorescence microscopies are generally used for micrometric sample regions at certain time points of biofilm development. *In situ* methods for the long-term monitoring of larger areas during biofilm formation and growth are therefore of high relevance in order to complement the state-of-the-art methods towards a deeper understanding of the processes involved.

* Corresponding authors.
E-mail addresses: hubert.girault@epfl.ch (H.H. Girault), andreas.lesch@unibo.it (A. Lesch).

One alternative approach to investigate biofilms is based on electrochemical methods that are increasingly applied for monitoring biofilms at the early stage of biofilm development [12]. Biofilm formation can, for instance, be followed by using electrochemical impedance spectroscopy [13], cyclic voltammetry [14], or chronoamperometry [15]. Besides biofilms, electrochemical methods have also been used to address single bacterial cells and bacterial cell aggregates [16–19]. Looking at the major advantages, electrochemical methods can reach high sensitivities while operating in small liquid volumes. Depending on the detection strategy, biofilms and bacterial cells can be analyzed without fixation. Electrochemical hardware can be made small and portable. The tolerance to optical perturbations is, in particular, advantageous over light-based detection methods. Electrochemical bioimaging that uses (sub)micrometric electrodes can be applied to study the electron transfer and the metabolic activity of biofilm samples [20]. Micrometer-resolved electrochemical imaging of biofilms can, on the one hand, be realized by placing biofilms onto two-dimensional microelectrode array chips [21,22]. On the other hand, an electrochemical scanning probe platform can be used, such as SECM, in which a micrometric electrochemical probe is translated in close proximity to a sample. It has, in particular, found applications for studying living cells [23, 24], yeast [25] and bacteria as well as biofilms [26–29]. Potential applications of biofilm analysis by SECM are diverse in terms of analytes to be detected and the type of bacteria under investigation [20,30]. Further, the combination of SECM with other techniques, such as SECM-atomic force microscopy [31] and SECM-fluorescence microscopy [32,33] or using other electrochemical scanning probe techniques alone, such as scanning ion conductance microscopy (SICM), gains interest for bacteria and biofilm studies [34]. The SECM signal can be an amperometric current as a result of the flux of the redox-active compounds generated or consumed by the bacterial cells [35–38]. For instance, the reduction of ferricyanide to ferrocyanide by the respiratory activity of *E. coli* cells was demonstrated and investigated by SECM [37,39]. SECM was further used to detect H_2O_2 at biofilms to study the glucose metabolism and catalase activity during the formation of *Streptococcus gordonii* biofilms [40]. Amperometric glucose micro-sensors have been applied as an example to detect selectively metabolites from *Streptococcus mutans* biofilms [41]. SECM has evolved into a widely used electroanalytical tool, often supported by data analysis based on analytical approximations, which allow the extraction of quantitative data, such as rate constants. However, when applied to biological systems [42–44], the complexity of the structure and morphology of biological samples complicates experimental procedures (*e.g.*, to guarantee the essential constant tip-to-sample-distance) and the interpretation of the data. One approach to simplify the experimental procedures is the application of soft contact mode microelectrodes (MEs) that were developed for Soft-Probe-SECM imaging of extremely delicate targets with irregular topographic features [45,46]. Using soft probes in contact mode, the working distance is kept constant without the implementation of specific hardware and software.

Herein, we present approach curves and electrochemical imaging of *E. coli* strain DH5α biofilms over square millimeter-sized sample regions using soft microelectrodes. Biofilms were grown and analyzed on different substrates and at different periods of biofilm development. The visualization of bacterial metabolic activity was based on the ability of the biofilm to reduce the oxidized form of ferrocene methanol. Soft-Probe-SECM electrochemical imaging was used to analyze various biofilm samples of bacteria with and without ampicillin-resistance as well as after gentamicin treatments.

2. Materials and methods

2.1. Materials

Ferrocene methanol (FcMeOH, 97 %), lysogeny broth (LB), 2xYT microbial growth medium, ampicillin, and gentamicin were bought from Sigma-Aldrich (St. Gallen, Switzerland). Phosphate buffered saline (PBS, 10 mM, pH 7.4) was prepared with disodium phosphate (Na_2HPO_4, 99.5 %), monosodium phosphate (NaH_2PO_4, 99.5 %), and sodium chloride (NaCl, ≥99 %), which were all purchased from Sigma-Aldrich (St. Gallen, Switzerland). Propidium iodide (PI) and SYTO 9 green-fluorescent nucleic acid stain were bought from Thermo Fisher Scientific company, USA. D-Squame adhesive sampling discs were bought from Clinical and Derm. *E. coli* strain DH5α and pBluescript SK II (+) were purchased from Invitrogen and Stratagene. All reagents and materials were of analytical grade and used as received. Deionized water was produced by a Milli-Q plus 185 model from Millipore (Zug Switzerland).

2.2. Biofilms and bacteria culture

2.2.1. Ampicillin resistant E. coli cells

E. coli DH5α cells were transformed with pBluescript SK II (+) conferring resistance to ampicillin. 50 µL of a solution with competent *E. coli* DH5α cells were incubated on ice with 10 ng of pBluescript plasmid DNA. Thereafter, a heat shock at 42 °C was applied for 45 s with subsequent incubation on ice for 2 min. The outgrowth of transformed bacteria was performed in LB by shaking (200 rpm) at 37 °C for 30 min. The cells were then distributed on LB agar plates containing 100 µg/mL ampicillin and incubated for 16 h at 37 °C. Finally, single bacterial colonies were picked to start suspension cultures and were grown for 12 16 h at 37 °C in LB containing 100 µg/mL ampicillin. This treatment affected all non-ampicillin-resistant bacteria and was used to avoid cross-contamination of *E. coli* with other bacteria in the environment.

2.2.2. Preparation of E. coli and ampicillin-resistant E. coli cell cultures

E. coli strain DH5α was grown as pre-cultures in LB at 37 °C for 6 h with continuous shaking at 200 rpm. 100 µL of each pre-culture was added into 900 µL of 2xYT and incubated overnight at 37 °C with constant shaking at 150 rpm. *E. coli* strain DH5α with resistance to ampicillin was also cultured in the same way as native *E. coli*, but the culture medium was enriched with a solution of 100 µg/mL ampicillin during all incubation steps. The obtained fresh cultures were afterward used for measurements of ampicillin-resistant *E. coli*.

2.2.3. Biofilm culture

4 mL of 5 mM $MgSO_4$ in 2xYT was added to the solution of *E. coli* DH5α cells (prepared in Section 2.2.2), which was incubated for 2 h under continuous shaking at 150 rpm. Glass slides were placed in culture dishes 60 (Thermo fisher scientific, Switzerland) and incubated overnight at 37 °C and 50 % humidity. The biofilm formed at the interface between the glass substrate surface and air and/or culture medium. The presence of Mg^{2+} in the medium positively affects the initial attachment of bacterial cells fostering biofilm formation [47] and increases the mechanical properties of the biofilms [48].

2.3. Tape stripping procedure and sample preparation

The biofilm-coated glass slides were removed from the culture dishes and air-dried. Adhesive tape was then pressed firmly onto the biofilms under slight lateral movements for several seconds to provide good adhesion before the tape was gently removed and further air-dried. This procedure removes the surface layer of the biofilm and fixes it on the adhesive (*vide infra*). The adhesive tape with the collected biofilm top-layer was fixed with double-side tape on a glass slide.

2.4. Antibiotic treatments for biofilm degradation

Antibiotic treatments were carried out for 1 h or 24 h of incubation in aqueous solutions with 32 µg/mL and 640 µg/mL of gentamicin. The biofilms were collected from the glass slides with adhesive tapes and transferred into the SECM setup (*vide infra*) (vide infra. Antibiotic

treatments were made on the tape-collected biofilms. After each antibiotic treatment and before each SECM measurement, *i.e.*, when the solutions were changed, the SECM cell was washed three times with DI water.

2.5. Characterization

2.5.1. Confocal laser scanning microscopy (CLSM)

A 20 μM solution of SYTO 9 was prepared from a 5 mM stock solution in DMSO by dilution with PBS. 300 μL of the solution was dropped on the biofilm-coated glass coverslip and incubated for 30 min at room temperature. The absorption wavelength and emission wavelength of SYTO 9 are 485 nm and 500 nm, respectively. Then, a 500 nM solution of PI was prepared by diluting a 1.5 mM stock solution in LB. 300 μL of the solution was dropped on the biofilm-coated glass coverslip and incubated for 5 min at room temperature. The absorption and emission wavelengths of PI are 535 nm and 617 nm, respectively. A Leica TCS SP8 white light laser (WLL) confocal microscope was used for visualization of the fluorescent markers.

2.5.2. Crystal violet staining

Biofilm-coated glass coverslips were washed three times with PBS and then dried at 60 °C for 15 min. The coverslips were afterwards incubated in 2 mL of 0.1 wt% crystal violet staining solution for 15 min. Thereafter, the coverslips were washed with PBS three times and dried at 60 °C for 15 min. Afterwards, the stained biofilm was immersed in 30 % acetic acid for 15 min to detach the stained biofilm from the glass slide. The solution was then analyzed with a Lambda 950S UV–vis spectrophotometer (PerkinElmer), and the results are given as optical density at 630 nm (OD_{630}).

2.5.3. Scanning electron microscopy (SEM)

Gold was sputtered with 6 nm thickness on a chromium pre-treated glass slide using a DP650 sputtering machine (Alliance-Concept). A biofilm was grown for one day on a gold-coated glass slide in the culture medium. Then, the Au-coated glass slide with biofilm on top was dried for 1 h in an incubator at 60 °C. The SEM images were acquired with a Thermo Scientific Teneo SEM at 5 kV accelerating voltage and using a beam current of 13 pA.

2.5.4. Other microscopy techniques

Laser scanning micrographs (LSM) were taken either with a Keyence VK-8700 laser scanning microscope or Axio Observer (Zeiss). Light micrographs were also taken by using a Dino-Lite digital microscope model AM4013MT.

2.5.5. Soft-Probe-SECM measurements

SECM measurements were carried out in a three-electrode configuration using a home-made SECM setup running under SECMx software (G. Wittstock, University of Oldenburg) and comprising a Compactstat (Ivium Technologies). A soft SECM probe containing a carbon paste microelectrode (ME, active electrode area ~100 μm2) acted as working electrode, a silver wire was used as quasi-reference electrode (QRE), and a platinum wire as counter electrode (CE). All potentials herein are referred to the QRE. The soft SECM probe (VersaSCAN (VS) Stylus, Princeton Applied Research – Ametek) was made of a thin and flexible PET sheet of 100 μm thickness. First, a microchannel was produced inside the PET sheet by laser ablation using an LSV3 excimer laser (Optec). Thereafter, the microchannels were three times filled with Electrador carbon ink (Electra Polymer & Chemicals Ltd.) with intermediate thermal curing at 80 ◦C for 1 h. Finally, the microchannels were sealed with a 2 μm thin Parylene C layer (Comelec SA, Switzerland). Before each experimental series, *i.e.*, for each fresh sample, the soft SECM probe tip was cut with a razor blade to provide a clean electrode surface. The soft SECM probe was brushed over the samples in a gentle contact mode with the Parylene C side touching the substrate. The probe was tilted by 20◦ in respect to the surface normal. Adhesive tapes were fixed with the collected sample directing upwards onto a microscope glass slide for stabilization and placed on the bottom of an electrochemical cell. All experiments were performed at room temperature (23 ± 2 °C).

Lateral SECM probe translations were carried out with a working electrode potential E_T = 0.5 V for the oxidation of FcMeOH, probe translation speed 25 μm/s, step size 10 μm and delay time between probe movement and current reading 0.1 s. The experimental solution contained 2.5 mM FcMeOH in 100 mM PBS with pH 7.4. To bring the SECM probe into contact with the substrate, a vertical probe movement was made until the soft probe touched the substrate.

3. Results and discussion

3.1. Optical characterization of biofilm surfaces

Biofilms of *E. coli* strain DH5α were grown *in vitro* on glass under static conditions. The presence of a biofilm was confirmed by using state-of-the-art microscopic techniques. Fig. 1a shows an exemplary biofilm of several square millimeters in lateral size. As it can be seen by the varying intensity of the white color, the biofilm contained regions with higher and lower density. Crystal violet staining visualized the presence of bacterial cells and extracellular polymeric substances (EPS) by turning the color of the biofilm violet (inset in Fig. 1a). CLSM of the biofilm was used to investigate the viability of *E. coli* cells (Fig. 1b-d, Supporting information SI-1). The continuous *z*-stack confocal bright-field image demonstrated the presence of a three-dimensional biofilm structure (Fig. 1b). Only a low number of bacterial cells moved within and near the biofilm, demonstrating that the major part of the bacterial cells was fixed in a matrix (Movie SI-1). SYTO 9/PI co-staining of nucleic acids was applied to distinguish live from dead bacterial cells (Fig. 1c,d). SYTO 9 is a green fluorescing, intercalating and membrane-permeable molecule that initially stains all bacterial cells, *i.e.*, live and dead cells. In contrast, PI is a red intercalating stain that is impermeable to membranes of intact bacteria. PI stains therefore only dead bacterial cells with damaged and porous cell membrane. As a result, green stains indicate all the bacterial cells (Fig. 1c, Movie SI-2) and red (here shown in yellow) stains indicate dead bacterial cells (Fig. 1d, Movie SI-3). The images suggest that the number of living bacterial cells was clearly higher than for dead bacterial cells indicating an intact biofilm. CTC/DAPI staining confirmed the results (SI-1, Movie SI-4). The SEM shows densely packed, multi-layered bacterial cells (Fig. 1e). A thin layer of the

VK-8700 laser scanning microscope or Axio Observer (Zeiss). Light mi-

EPS matrix covered and connected individual bacterial cells and crographs were also taken by using a Dino-Lite digital microscope model AM4013MT.

3.1.1. Soft-Probe-SECM measurements

SECM measurements were carried out in a three-electrode configuration using a home-made SECM setup running under SECMx software (G. Wittstock, University of Oldenburg) and comprising a Compactstat (Ivium Technologies). A soft SECM probe containing a carbon paste microelectrode (ME, active electrode area ~100 μm^2) acted as working electrode, a silver wire was used as quasi-reference electrode (QRE), and a platinum wire as counter electrode (CE). All potentials herein are referred to the QRE. The soft SECM probe (VersaSCAN (VS) Stylus, Princeton Applied Research – Ametek) was made of a thin and flexible PET sheet of 100 μm thickness. First, a microchannel was produced inside the PET sheet by laser ablation using an LSV3 excimer laser (Optec). Thereafter, the microchannels were three times filled with Electrador carbon ink (Electra Polymer & Chemicals Ltd.) with intermediate thermal curing at 80 °C for 1 h. Finally, the microchannels were sealed with a 2 μm thin Parylene C layer (Comelec SA, Switzerland). Before each experimental series, *i.e.*, for each fresh sample, the soft SECM probe tip was cut with a razor blade to provide a clean electrode surface. The soft SECM probe was brushed over the samples in a gentle contact mode with the Parylene C side touching the substrate. The probe was tilted by 20°

confirmed further the presence of a biofilm (Fig. 1f, SI-2).

3.2. SECM feedback mode characterization of E. coli biofilm surfaces

Soft-Probe-SECM (SI-3) in feedback mode was carried out in 100 mM PBS (pH 7.4) using 2.5 mM FcMeOH as redox mediator in order to investigate the electrochemical surface reactivity of a biofilm and the possibility of electrochemical biofilm imaging. In fact, the reduction of Fe^{III}-containing species, which compete with oxygen as terminal electron acceptors within the respiratory electron transport chain (ETC) in *E. coli* cells, was previously reported [49]. In this work, $FcMeOH^+$ (Fe^{III}) is generated by electrochemical oxidation of FcMeOH at the soft ME from where it then diffuses towards the sample (Fig. 2a). Compared to a soft probe in solution bulk (probe height h_P =1 mm), the SECM currents are lower when the soft probe is in physical contact ($h_P \leq 0$ μm) with biofilm-free, insulating sample regions. The diffusion of FcMeOH from the solution bulk is physically hindered by the substrate ("negative feedback"). FcMeOH reaches the soft microelectrode only through the tiny gap between microelectrode and sample, leading to the remaining recorded current (Fig. 2a). When the soft probe touched a glass slide, it started sliding forward with a nearly constant working distance, which becomes clear by the nearly constant SECM current for $h_P < 0$ μm ($I_{Norm,\ glass} < 0.20$, black curve in Fig. 2b). For the approach curves in Fig. 2, the

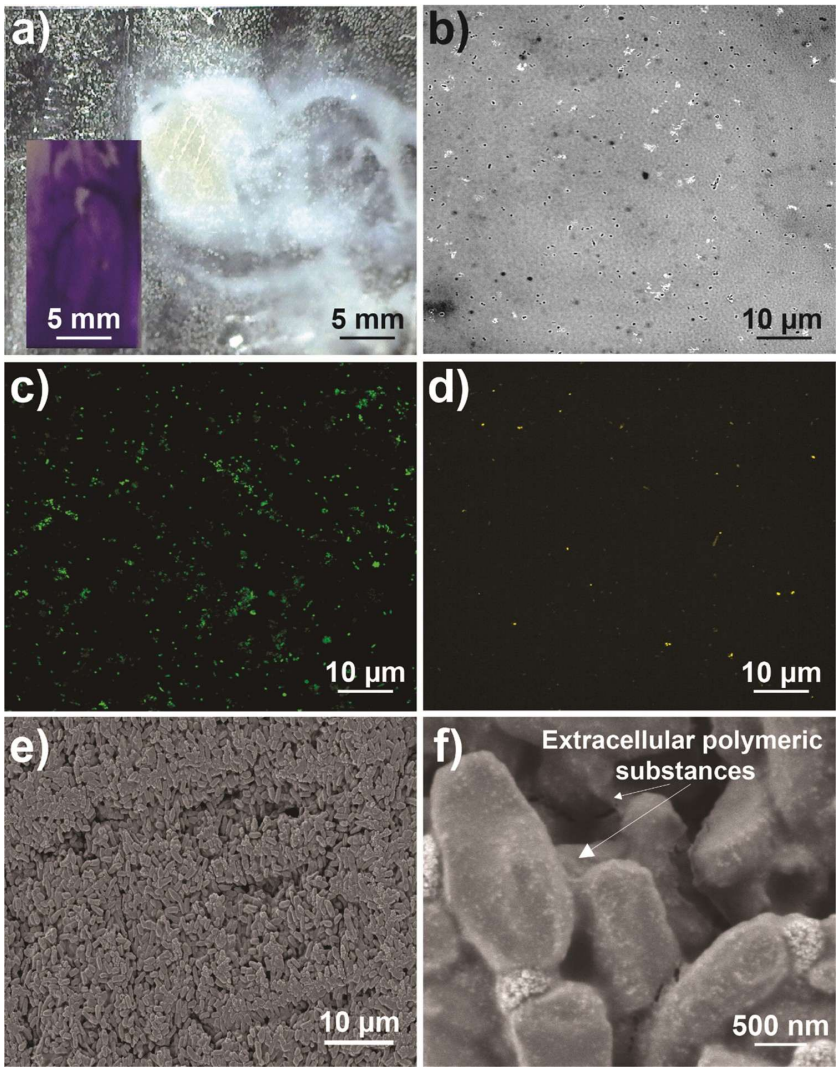

Fig. 1. Optical microscopy of an *E. coli* biofilm that was grown for one day on a glass slide. (a) Light micrographs before (main figure) and after (inset) viability testing using crystal violet staining. (Note: two different samples). CLSM bright-field (b) and fluorescence micrographs (c,d). (c) SYTO 9 staining (all bacteria). (d) PI staining (dead bacteria). (e-f) SEM images with two different magnifications. Each analysis was done with a fresh biofilm.

SECM currents I were normalized by the current recorded in the solution bulk I_{Bulk} giving in the bulk $I_{Norm,bulk} = 1$. In contrast, approaching the soft microelectrode towards an one-day-old *E. coli* biofilm on glass resulted at the contact point between soft probe and biofilm in a feedback current significantly larger than over bare glass ($I_{Norm,biofilm/glass} = 0.88$, Fig. 2b, c). This could be due to the ability of the biofilm to reduce $FcMeOH^+$ back to FcMeOH, for instance, within the respiratory electron transport chain of metabolically active *E. coli* cells (redox potential of FcMeOH -0.44 V *vs* SHE) [50]. The electrochemical reactivity of the biofilm results in an additional flux of FcMeOH from the *E. coli* cells embedded in the biofilm and thus towards the soft microelectrode. The SECM current over the biofilm on glass was up to eight times higher than over bare glass (Fig. 2b), but lower than the steady-state dif-fusion-controlled current for the oxidation of FcMeOH in the solution bulk ($I_{Norm,bulk}$ 1). This suggests finite kinetics for the regeneration reaction in the biofilm and/or limited mass transport within the biofilmmatrix, as well as, across the bacterial cell membranes. In the literature, approach curves with decaying feedback current using FcMeOH as a redox mediator were reported to locate the surface of *E. coli* biofilms [51]. However, the diffusion of FcMeOH from the solution bulk within the biofilm matrix and reaching also in this way the microelectrode as an additional flux from the bottom could principally contribute to the signal (the water content in biofilms can be up to 97 %, [52]). It would depend on the thickness of the biofilm and also on the size of available diffusion channels in the three-dimensional biofilm structure (herein the biofilm thickness was below 10 µm when dry, SI-4). Finally, also redox activity of the extracellular matrix and biofilm microenvironment (*e.g.* by the release of redox-active molecules) could contribute to the signal, but the release of compounds, such as, for instance, quorum-sensing molecules, plays a larger role in other bacterial species than *E. coli* [19,38,53,54]. Approach curves were then performed over three identically grown *E. coli* biofilms on three glass slides ($N_{Sample} = 3$, Fig. 2b) in duplicate and laterally separated by 100 µm (six approach curves in total). The normalized feedback current at the contact point between

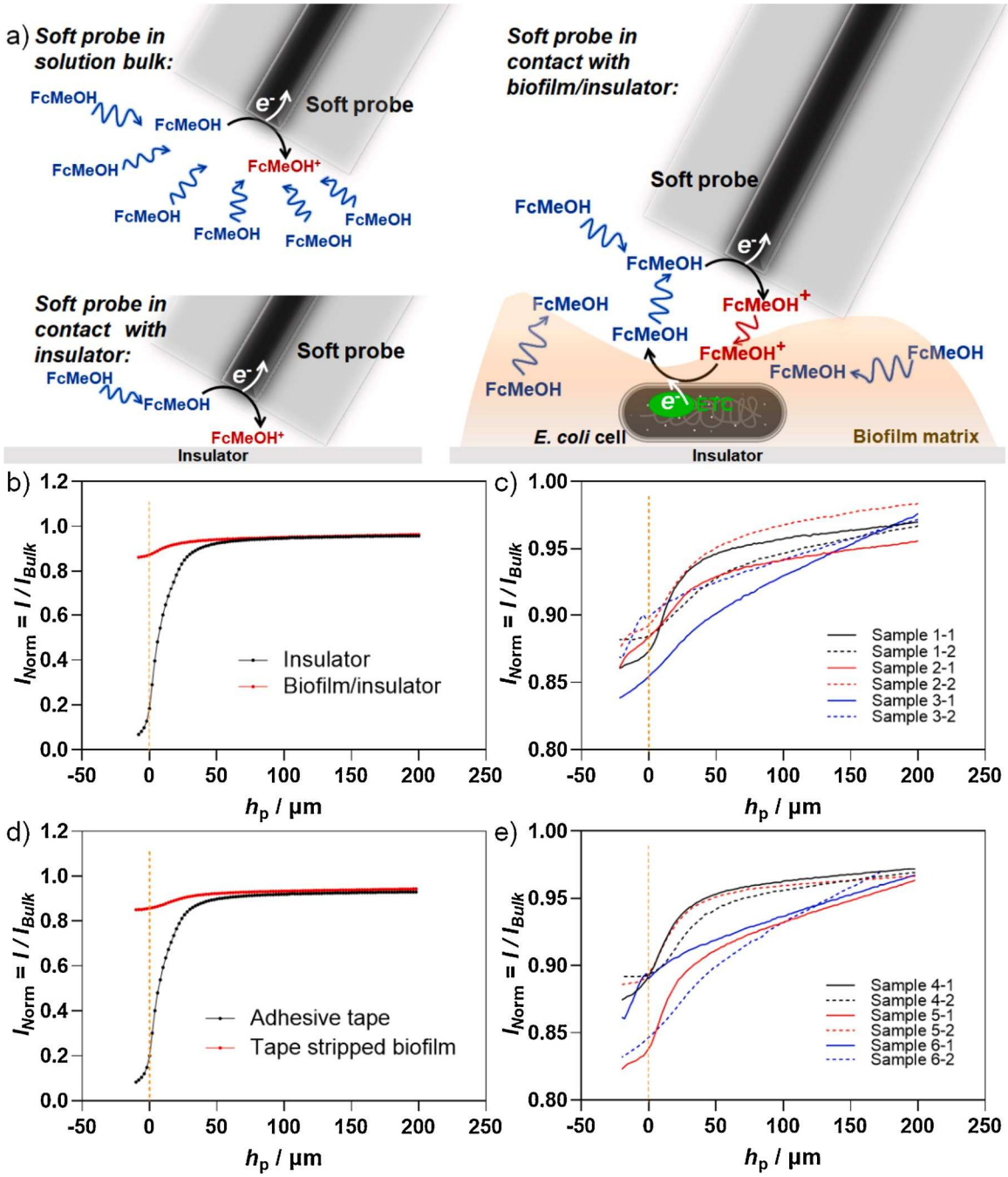

Fig. 2. SECM feedback mode approach curves over one-day-old *E. coli* biofilm-coated and biofilm-free glass and adhesive tape substrates. (a) Schematic repre- sentation of the "unhindered", nearly hemispherical diffusion of FcMeOH towards the microelectrode with the soft probe in the solution bulk ($I_{Norm,bulk}$ = 1), hindered diffusion when the soft probe is near or in contact with a smooth insulator like glass ($I_{Norm,insulator}$ = →0), hindered diffusion with redox mediator regeneration when the soft probe contacts the biofilm ($I_{Norm,insulator}$ < $I_{Norm,biofilm/insulator}$ < $I_{Norm,bulk}$). (b) Approach curves over glass and biofilm/glass. (c) Two locally separated approach curves over each of three identically grown biofilms on glass (N_{Sample} = 3). (d) Approach curves over adhesive tape and tape-stripped biofilm surface layer on adhesive tape. (e) Two locally separated approach curves over each of three identically grown, tape-stripped biofilm surface layers on adhesive tape (N_{Sample} = 3). Experimental details: E_T = 0.5 V, probe translation speed =5 µm/s, step size =2 µm, 2.5 mM FcMeOH in 100 mM PBS (pH = 7.4).

soft probe and sample for all six approach curves over the biofilm was ~0.87 and varied by 2.3 % (Fig. 2c). This suggests repeatability for the biofilm growth protocol, as well as, for the feedback mode approach curves. After that, three identically grown biofilms on glass were tape-stripped with an adhesive tape (N_{Sample} = 3). This procedure removes few micrometers (determined as (2.2± 1.1) µm when dry, SI-4) of the biofilm surface demonstrating the possibility of collecting biofilm surface layers from any surface of interest for analysis using Soft-Probe-SECM. Notably, the approach curves over bare adhesive tape and tape-collected biofilm surface layers resulted in very similar feedback mode currents compared to bare glass and the entire biofilms on glass, respectively. The normalized currents at the contact points between the soft probe and the biofilm-free adhesive layer were $I_{Norm,adhesive}$ = 0.2 and with the tape-collected biofilm surface $I_{Norm,biofilm\ surface/adhesive}$ =0.86 (Fig. 2d). This was verified for a total of six approach curves on the three different samples (Fig. 2e). These results suggest that the sensitivity of the SECM feedback mode is restricted to the surface layer of the biofilm. Therefore, the SECM approach operates

in a surface confined mode and enables the analysis of biofilm surface layers on entire biofilms as well as on tape-collected biofilm surface layers.

Thereafter, an *E. coli* biofilm, grown for one day on a glass slide, was partially cleared using a soft wipe wetted with alcohol to create a sample with an almost sharp biofilm-glass border for SECM feedback mode imaging (Fig. 3a-b). The sample was air-dried at room temperature for 15 min before it was covered with 2.5 mM FcMeOH containing solution in 100 mM PBS (pH 7.4). A soft probe was repeatedly placed with continuous perpendicular displacements onto the glass part and horizontally translated over the biofilm-coated region constructing the SECM feedback mode image in Fig. 3c. As expected, the SECM feedback mode currents over the biofilm were higher than over glass suggesting that $FcMeOH^+$ was reduced by the biofilm-coated region. The mean SECM current over the glass was generally (0.09 ± 0.04) nA and (0.70 ± 0.24) nA on the biofilm-coated site. The presence of a few remaining active bacterial cells and biofilm (Fig. 3b) on the cleaned glass side most likely could not contribute to the SECM signal due to the sensitivity limits of the used probe. The integrity of the biofilm and thus the ability to regenerate metabolically the redox mediator could have been influenced by the nearby alcohol treatment. In conclusion, the biofilm during consecutive contact mode line scanning remained adhered and the active part of the soft probe did not get contaminated by biofilm material as seen by its stable response.

3.3. Feedback mode imaging of biofilm formation with ampicillin-resistant or -susceptible DH5α E. coli cells

Biofilm formation is a stepwise process: (1) attachment of bacterial cells to a substrate surface, (2) maturation of the biofilm (formation of a viable 3D structure), and (3) partial dispersion/detachment of biofilm components (bacterial cells are released from biofilm regions with less nutrient supply). Crystal violet staining (SI-5) was first carried out daily on ten separately grown ampicillin-susceptible *E. coli* biofilms on glass (N_{Sample} 10, Fig. 4a(ii)). Ampicillin-susceptible bacterial cells formed biofilms without ampicillin protection against co-bacterial contamination. An overall increase of the total biofilm mass was detected by the increasing OD_{630nm} leading to a sigmoidal shape of the OD_{630nm} value as a function of culturing time, approaching a quasi-plateau at day six (Fig. 4b). This quasi-plateau could indicate a continuous growth of the biofilm with continuous detachment of daily similar amounts of biofilm material. Based on the conclusions made in the previous section, *i.e.*, tape-stripped biofilm surface layers give similar SECM signals as the direct analysis of the surface layers of entire biofilms, the top layer of one biofilm for each of the ten samples with progressing growth period was collected with adhesive tape and then analyzed by SECM feedback mode imaging (Fig. 4a(i)). The SECM feedback mode images indicate local variations in current over lateral dimensions of about 50 µm–100 µm. These features are repeatedly observed, as, for instance, seen by repeatedly recorded SECM line scans (SI-6). This could be due to the morphology of the adhesive tape after sample collection and by mounting the tape in the SECM cell. The tape morphology could affect probe sliding and probe angle, but was not seen in our previous work [44]. Further, variations in local biofilm collection efficiency of the adhesive layer could affect the biofilm coverage on the tape. Finally, signal variations could be the result of a yet to be confirmed intrinsic heterogeneous metabolic activity of the biofilm. Features of similar dimensions can be seen in the images of crystal violet stained biofilms from Day 6 to Day 9. It is part of ongoing work to understand whether these features could be linked to those seen in the SECM images. The mean feedback mode current was calculated for each SECM image (1 mm^2) using all 10'251 data points per image. To compensate for possible variations between SECM experiments in terms of the exact soft probe dimension after mechanical cutting and the exact probe angle [44, 46], the mean soft probe responses were calibrated by considering the bulk current and negative feedback current over an insulator (SI-7). The mean SECM feedback mode current during SECM imaging of the biofilm-coated adhesive layer (one day biofilm growth) was ten times

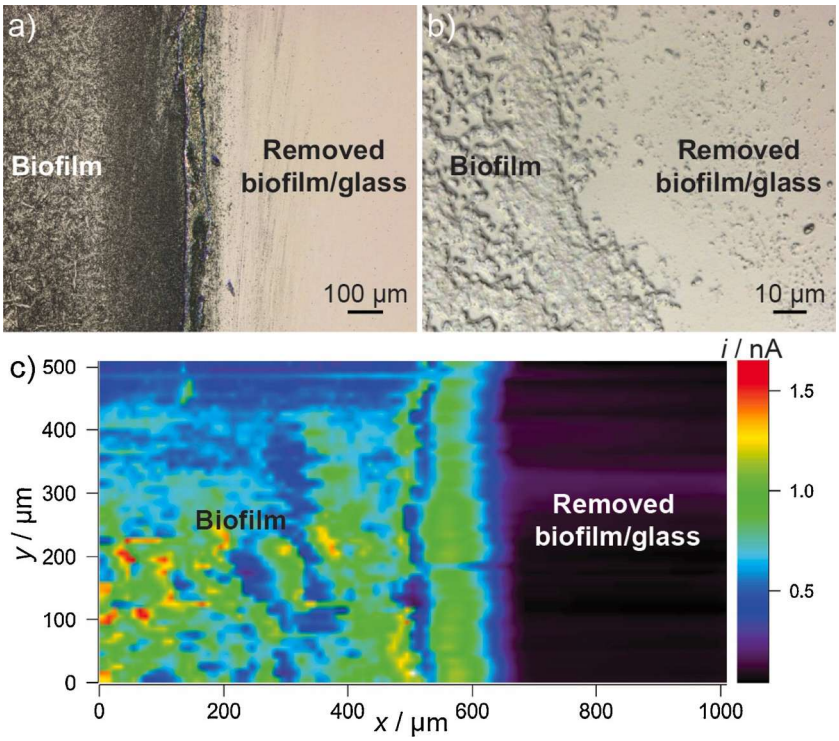

Fig. 3. Soft-Probe-SECM imaging of *E. coli* biofilm on glass. (a,b) LSMs of the biofilm with two magnifications. (c) Soft-Probe-SECM feedback mode image of an *E. coli* biofilm-glass border, generated with an alcohol-soaked wipe. Considered biofilm area = 0.5 mm^2. Experimental details: E_T = 0.5 V, probe translation speed =25 µm/s, step size =10 µm, 2.5 mM FcMeOH in 100 mM PBS (pH = 7.4).

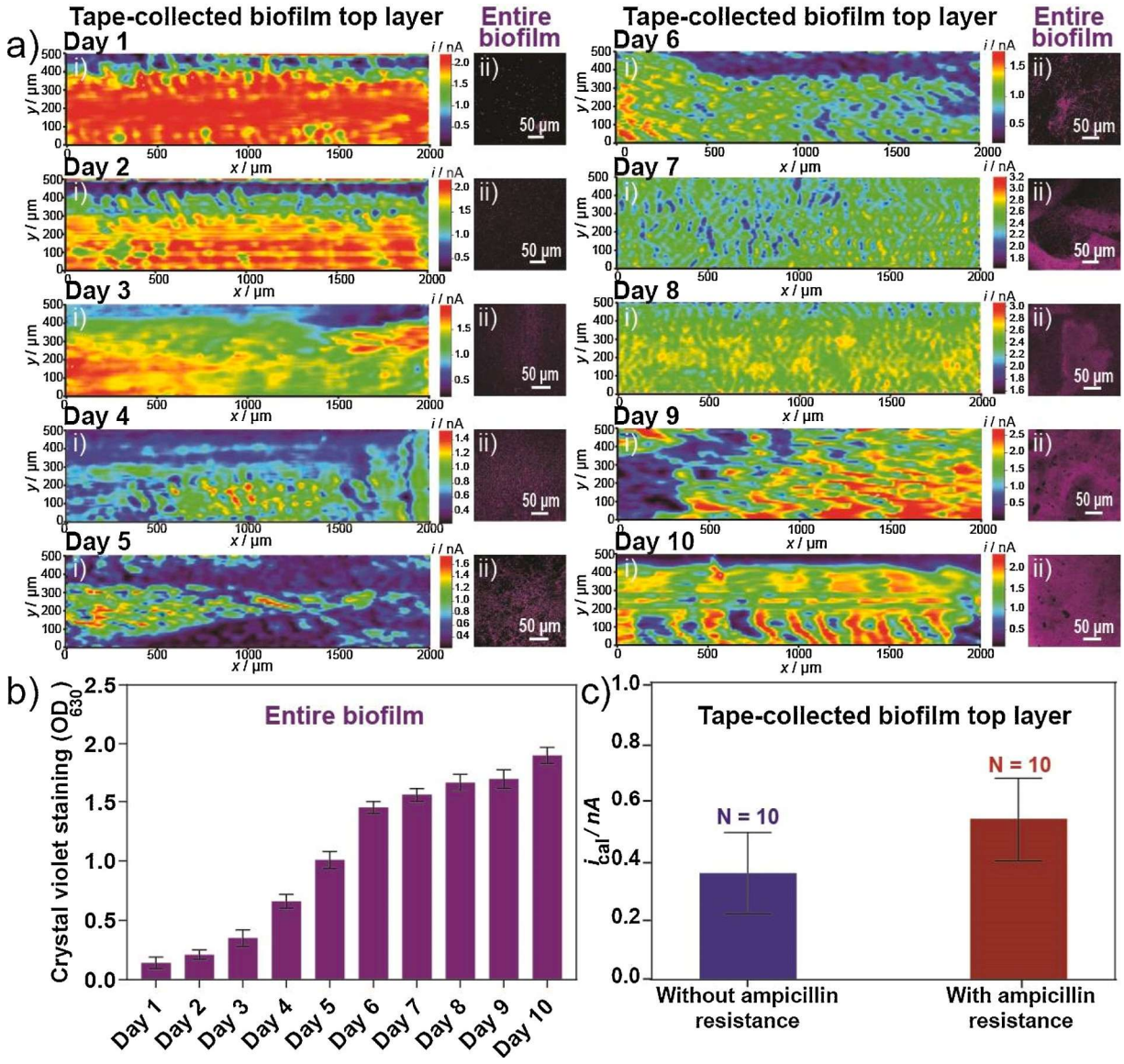

Fig. 4. SECM imaging and crystal violet staining of the surface layers of *E. coli* biofilms and entire biofilms, respectively, during biofilm formation over ten days. (a) (i) Soft-probe SECM feedback mode images of tape-collected biofilm surface layers and (ii) fluorescence images of entire crystal violet stained biofilms on glass. (b) OD_{630} of crystal violet-stained total biomass of *E. coli* biofilms after removal from glass. (c) Mean currents ± standard deviation of ten biofilms with *E. coli* without and with ampicillin resistance. Experimental SECM details: E_T = 0.5 V, probe translation speed =25 µm/s, step size =10 µm, 2.5 mM FcMeOH in 100 mM PBS (pH = 7.4). Reported SECM imaging area: 1 mm^2.

higher ((1.73 0.54) nA (SI-8) than the current over bare adhesive tape (0.17 0.05) nA (SI-9). As the SECM detection sensitivity seems to be surface-confined, the mean currents of the SECM images of the tape-collected top biofilm layer over ten days cannot follow the same trend as the increasing OD_{630nm} intensities of crystal violet stained entirebiofilm mass on glass. The mean SECM current of the measurement se-ries with ampicillin-susceptible *E. coli* biofilms was calculated and compared with the mean current of the ten images taken daily during the growth of ten separate ampicillin-resistant *E. coli* biofilms (grown inthe presence of ampicillin, (SI-10)). The lower calibrated mean current of (0.36 0.14) nA *versus* (0.54 0.14) nA could suggest that the use ofampicillin-resistant *E. Coli* resulted in a biofilm with higher metabolic activity (Fig. 4c).

3.4. SECM imaging of E. coli biofilm during antibiotic treatment

Gentamicin is one of the most effective antibiotics against *E. coli* biofilms [55]. It is an aminoglycoside-based hydrophobic compound that permeates through the outer membrane of *E. coli* cells [56]. The effectiveness of aminoglycosides is based on the inhibition of the synthesis of proteins through binding to the 30S ribosome. A second lethal effect could be the perturbation of the surface of the bacterial cells [55]. Herein, the minimum inhibitory concentration (MIC) of 32 µg/mL gentamicin was applied for 1 h (Fig. 5a) and 24 h (Fig. 5b) to two tape-collected *E. coli* biofilms. Thereafter, 20 times the MIC (20 MIC = 640 µg/mL) was applied for 1 h (Fig. 5c) to a third tape-collected *E. coli* biofilm [57]. For all of the three cases, SECM imaging of the same areas was carried out before and after the antibiotic treatment. The two solutions with FcMeOH and the antibiotic were changed and the samples washed. After antibiotic treatment, the SECM FB currents over the biofilms decreased, however, to a different extend. At the MIC, the mean SECM current decreased by 80 % after 1 h and 94 % after 24 h. Therefore, it can be concluded that only little biofilm activity remained. After 1 h with 20 MIC, the activity of the biofilms was nearly completely reduced (*i.e.*, 99 %). As expected, the antibiotic treatment was more efficient with longer treatment times and with higher antibiotic

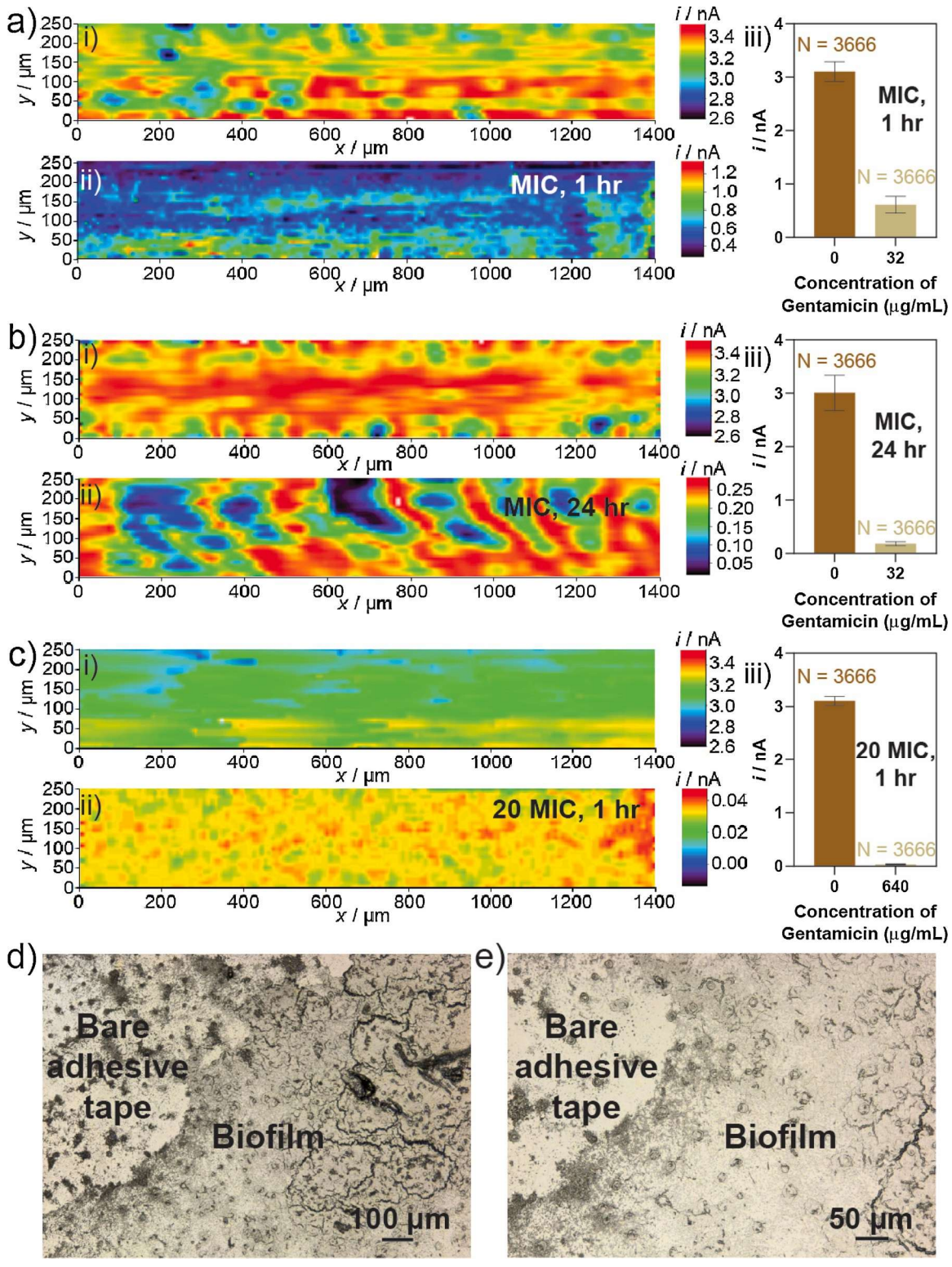

Fig. 5. Soft-Probe-SECM imaging of tape-collected one-day-old, ampicillin-resistant *E. coli* biofilm before (i) and after (ii) gentamicin treatment. (a) 32 μg/mL (MIC), incubation time =1 h. (b) 32 μg/mL (MIC), incubation time =24 h. (c) 640 μg/mL (20 MIC), incubation time =1 h. (a-c, iii) Mean SECM FB currents ± standard deviation. (d) and (e) LSMs of one *E. coli* biofilm after the gentamicin treatment with 20 MIC and an incubation time of 1 h in two magnifications. Experimental SECM details: E_T = 0.5 V, probe translation speed =25 μm/s, step size =10 μm, 2.5 mM FcMeOH in 100 mM PBS (pH = 7.4).

concentration. LSMs of the biofilms after (Fig. 5d,e) antibiotic treatment with 20 MIC demonstrated the presence of the structure of remaining biofilm on the tape.

4. Conclusion

In this work, the electrochemical surface reactivity of *E. coli* biofilms was investigated using Soft-Probe-SECM in feedback mode. First, the formation of *E. coli* biofilms was confirmed by using standard

microscopic methods. FcMeOH was used as a redox indicator for visualizing the presence of biofilms electrochemically. The *E. coli* biofilms showed the ability to reduce $FcMeOH^+$ and enabled SECM feedback mode characterization and imaging. Soft microelectrodes were gently brushed over the biofilm allowing scanning experiments with a nearly constant working distance while keeping the biofilm intact. Biofilms were analyzed on glass slides and their top surface layer of ~2 μm thickness after collection with adhesive tapes. As the responses of both systems appeared very similar, the SECM method appeared sensitive to the surface layer of the biofilms. The micro-electrochemical imaging procedure was repeated during several days of biofilm growth and could distinguish the growth of ampicillin-susceptible and -resistant *E. coli* biofilms. Finally, this work demonstrated that Soft-Probe-SECM imagingis a powerful tool to analyze the degradation of biofilms in the presenceof antimicrobial agents such as antibiotics. The work demonstrated that FcMeOH is a suitable redox indicator of biofilms for general and long-lasting biofilm studies with accessible metabolic activity in the surface layer. The technique complements microscopic techniques, gene expression analysis, and proteomics, and could open the door for further SECM-based biofilm studies. The work is currently extended to other than model biofilms and different SECM detection concepts.

CRediT authorship contribution statement

Sorour Darvishi: Methodology, Investigation, Validation, Visualization, Writing - original draft, Writing - review & editing. **Horst Pick:** Resources, Investigation, Writing - review & editing. **Emad Oveisi:** Investigation. **Hubert H. Girault:** Resources, Conceptualization, Supervision. **Andreas Lesch:** Conceptualization, Supervision, Writing - review & editing.

Declaration of Competing Interest

The authors declare that they have no known competing financial interests or personal relationships that could have appeared to influence the work reported in this paper.

Appendix A. Supplementary data

References

[1] M. Jamal, W. Ahmad, S. Andleeb, F. Jalil, M. Imran, M.A. Nawaz, T. Hussain, M. Ali, M. Rafiq, M.A. Kamil, Bacterial biofilm and associated infections, J. Chin. Med. Assoc. 81 (2018) 7–11, https://doi.org/10.1016/j.jcma.2017.07.012.

[2] Z. Khatoon, C.D. McTiernan, E.J. Suuronen, T.F. Mah, E.I. Alarcon, Bacterial biofilm formation on implantable devices and approaches to its treatment and prevention, Heliyon 4 (2018), e01067, https://doi.org/10.1016/j.heliyon.2018.e01067.

[3] G. Gebreyohannes, A. Nyerere, C. Bii, D.B. Sbhatu, Challenges of intervention, treatment, and antibiotic resistance of biofilm-forming microorganisms, Heliyon 5 (2019), e02192, https://doi.org/10.1016/j.heliyon.2019.e02192.

[4] P.S. Stewart, M.J. Franklin, Physiological heterogeneity in biofilms, Nat. Rev. Microbiol. 6 (2008) 199–210, https://doi.org/10.1038/nrmicro1838.

[5] T. Bjarnsholt, The role of bacterial biofilms in chronic infections, Apmis 121 (2013) 1–58, https://doi.org/10.1111/apm.12099.

[6] P. Neopane, H.P. Nepal, R. Shrestha, O. Uehara, Y. Abiko, In vitro biofilm formation by Staphylococcus aureus isolated from wounds of hospital-admitted patients and their association with antimicrobial resistance, Int. J. Gen. Med. 11 (2018) 25–32, https://doi.org/10.2147/IJGM.S153268.

[7] N. Sabir, A. Ikram, G. Zaman, L. Satti, A. Gardezi, A. Ahmed, et al., Bacterial biofilm-based catheter-associated urinary tract infections: causative pathogens and antibiotic resistance, Am. J. Infect. Control 45 (2017) 1101–1105, https://doi.org/10.1016/j.ajic.2017.05.009.

[8] C. Vuotto, F. Longo, C. Pascolini, G. Donelli, M. Balice, M. Libori, et al., Biofilm formation and antibiotic resistance in Klebsiella pneumoniae urinary strains, J. Appl. Microbiol. 123 (2017) 1003–1018, https://doi.org/10.1111/jam.13533.

[9] O. Fysun, H. Kern, B. Wilke, H.-C. Langowski, Evaluation of factors influencing dairy biofilm formation in filling hoses of food-processing equipment, Food Bioprod. Process 113 (2019) 39–48, https://doi.org/10.1016/j.fbp.2018.10.009.

[10] C. Reichhardt, M.R. Parsek, Confocal laser scanning microscopy for analysis of Pseudomonas aeruginosa biofilm architecture and matrix localization, Front. Microbiol. 10 (2019) 677, https://doi.org/10.3389/fmicb.2019.00677.

[11] Y. Chao, T. Zhang, Optimization of fixation methods for observation of bacterial cell morphology and surface ultrastructures by atomic force microscopy, Appl. Microbiol. Biotechnol. 92 (2011) 381–392, https://doi.org/10.1007/s00253-011-3551-5.

[12] G. Li, Y. Wu, Y. Li, Y. Hong, X. Zhao, P.I. Reyes, et al., Early stage detection of Staphylococcus epidermidis biofilm formation using MgZnO dual-gate TFT biosensor, Biosens. Bioelectron. 151 (2020) 111993, https://doi.org/10.1016/j.bios.2019.111993.

[13] D. Naradasu, A. Guionet, W. Miran, A. Okamoto, Microbial current production from Streptococcus mutans correlates with biofilm metabolic activity, Biosens. Bioelectron. 162 (2020) 112236, https://doi.org/10.1016/j.bios.2020.112236.

[14] X. Liu, S. Zhuo, X. Jing, Y. Yuan, C. Rensing, S. Zhou, Flagella act as Geobacter biofilm scaffolds to stabilize biofilm and facilitate extracellular electron transfer, Biosens. Bioelectron. 146 (2019) 111748, https://doi.org/10.1016/j.bios.2019.111748.

[15] B. Abada, S. Boumerfeg, A. Haddad, M. Etienne, Electrochemical investigation of Thiobacillus denitrificans in a bacterial composite, J. Electrochem. Soc. 167 (2020) 135502, https://doi.org/10.1149/1945-7111/abbdd7.

[16] S. Nara, R. Kandpal, V. Jaiswal, S. Augustine, S. Wahie, J.G. Sharma, et al., Exploring Providencia rettgeri for application to eco-friendly paper based microbial fuel cell, Biosens. Bioelectron. 165 (2020) 112323, https://doi.org/10.1016/j.bios.2020.112323.

[17] Y. Zhu, M. Jović, A. Lesch, L. Tissières Lovey, M. Prudent, H. Pick, et al., Immuno-affinity amperometric detection of bacterial infections, Angew. Chem. Int. Ed. 57 (2018) 14942–14946, https://doi.org/10.1002/anie.201808666.

[18] O. Simoska, K.J. Stevenson, Electrochemical sensors for rapid diagnosis of pathogens in real time, Analyst 144 (2019) 6461–6478, https://doi.org/10.1039/C9AN01747J.

[19] J.L. Connell, J. Kim, J.B. Shear, A.J. Bard, M. Whiteley, Real-time monitoring of quorum sensing in 3D-printed bacterial aggregates using scanning electrochemical microscopy, PNAS 111 (2014) 18255–18260, https://doi.org/10.1073/pnas.1421211111.

[20] G. Caniglia, C. Kranz, Scanning electrochemical microscopy and its potential for studying biofilms and antimicrobial coatings, Anal. Bioanal. Chem. 412 (2020) 6133–6148, https://doi.org/10.1007/s00216-020-02782-7.

[21] D.L. Bellin, H. Sakhtah, Y. Zhang, A. Price-Whelan, L.E. Dietrich, K.L. Shepard, Electrochemical camera chip for simultaneous imaging of multiple metabolites in biofilms, Nat. Commun. 7 (2016) 1–10, https://doi.org/10.1038/ncomms10535.

[22] L. Liu, Y. Xu, F. Cui, Y. Xia, L. Chen, X. Mou, et al., Monitoring of bacteria biofilms forming process by in-situ impedimetric biosensor chip, Biosens. Bioelectron. 112 (2018) 86–92, https://doi.org/10.1016/j.bios.2018.04.019.

[23] J. Zhang, T. Zhu, J. Lang, W. Fu, F. Li, Recent advances of scanning electrochemical microscopy and scanning ion conductance microscopy for single cell analysis, Curr. Opin. Electrochem. 22 (2020) 178–185, https://doi.org/10.1016/j.coelec.2020.06.001.

[24] J. Petroniene, I. Morkvenaite-Vilkonciene, R. Miksiunas, D. Bironaite, A. Ramanaviciene, K. Rucinskas, V. Janusauskas, A. Ramanavicius, Scanning electrochemical microscopy for the investigation of redox potential of human myocardium-derived mesenchymal stem cells grown at 2D and 3D conditions, Electrochim. Acta 360 (2020) 136956, https://doi.org/10.1016/j.electacta.2020.136956.

[25] A. Valiūnienė, J. Petronienė, M. Dulkys, A. Ramanavičius, Investigation of active and inactivated yeast cells by scanning electrochemical impedance microscopy, Electroanalysis 32 (2020) 367–374, https://doi.org/10.1002/elan.201900414.

[26] R. Borghese, M. Malferrari, M. Brucale, L. Ortolani, M. Franchini, S. Rapino, F. Borsetti, D. Zannoni, Structural and electrochemical characterization of lawsone-dependent production of tellurium-metal nanoprecipitates by photosynthetic cells of Rhodobacter capsulatus, Bioelectrochemistry 133 (2020) 107456, https://doi.org/10.1016/j.bioelechem.2020.107456.

[27] C.S. Santos, F. Macedo, A.J. Kowaltowski, M. Bertotti, P.R. Unwin, F.M. da Cunha, G.N. Meloni, Unveiling the contribution of the reproductive system of individual Caenorhabditis elegans on oxygen consumption by single-point scanning electrochemical microscopy measurements, Anal. Chim. Acta 1146 (2021) 88–97, https://doi.org/10.1016/j.aca.2020.12.030.

[28] E. Abucayon, N. Ke, R. Cornut, A. Patelunas, D. Miller, M.K. Nishiguchi, C.G. Zoski, Investigating catalase activity through hydrogen peroxide decomposition by bacteria biofilms in real time using scanning electrochemical microscopy, Anal. Chem. 86 (2014) 498–505, https://doi.org/10.1021/ac402475m.

[29] D. Rudolph, D. Bates, T.J. DiChristina, B. Mizaikoff, C. Kranz, Detection of metal-reducing enzyme complexes by scanning electrochemical microscopy, Electroanalysis 28 (2016) 2459–2465, https://doi.org/10.1002/elan.201600333.

[30] S.E. Darch, D. Koley, Quantifying microbial chatter: scanning electrochemical microscopy as a tool to study interactions in biofilms, Proc. R. Soc. A 474 (2018) 20180405, https://doi.org/10.1098/rspa.2018.0405.

[31] S. Daboss, J. Lin, M. Godejohann, C. Kranz, Redox switchable polydopamine-modified AFM-SECM probes: a probe for electrochemical force spectroscopy, Anal. Chem. 92 (2020) 8404–8413, https://doi.org/10.1021/acs.analchem.0c00995.

[32] L. Guerret-Legras, J.F. Audibert, G.V. Dubacheva, F. Miomandre, Combined scanning electrochemical and fluorescence microscopies using a tetrazine as a single redox and luminescent (electrofluorochromic) probe, Chem. Sci. 9 (2018) 5897–5905, https://doi.org/10.1039/c8sc01814f.

[33] L. Guerret-Legras, J.F. Audibert, I.G. Ojeda, G.V. Dubacheva, F. Miomandre, Combined SECM-fluorescence microscopy using a water-soluble

electrofluorochromic dye as the redox mediator, Electrochim. Acta 305 (2019) 370–377, https://doi.org/10.1016/j.electacta.2019.03.069.
[34] K. Cremin, B.A. Jones, J. Teahan, G.N. Meloni, D. Perry, C. Zerfass, M. Asally, O. S. Soyer, P.R. Unwin, Scanning ion conductance microscopy reveals differences in the ionic environments of gram-positive and negative bacteria, Anal. Chem. 92 (2020) 16024–16032, https://doi.org/10.1021/acs.analchem.0c03653.
[35] S.E. Darch, D. Koley, Quantifying microbial chatter: scanning electrochemical microscopy as a tool to study interactions in biofilms, Proc. R. Soc. A 474 (2018) 20180405, https://doi.org/10.1098/rspa.2018.0405.
[36] C. Cai, B. Liu, M.V. Mirkin, H.A. Frank, J.F. Rusling, Scanning electrochemical microscopy of living cells. 3. Rhodobacter sphaeroides, Anal. Chem. 74 (2002) 114–119, https://doi.org/10.1021/ac010945e.
[37] T. Kaya, D. Numai, K. Nagamine, S. Aoyagi, H. Shiku, T. Matsue, Respiration activity of Escherichia coli entrapped in a cone-shaped microwell and cylindrical micropore monitored by scanning electrochemical microscopy (SECM), Analyst 129 (2004) 529–534, https://doi.org/10.1039/b316582e.
[38] D. Koley, M.M. Ramsey, A.J. Bard, M. Whiteley, Discovery of a biofilm electrocline using real-time 3D metabolite analysis, PNAS 108 (2011) 19996–20001, https://doi.org/10.1073/pnas.1117298108.
[39] G. Gao, D. Wang, R. Brocenschi, J. Zhi, M.V. Mirkin, Toward the detection and identification of single bacteria by electrochemical collision technique, Anal. Chem. 90 (2018) 12123–12130, https://doi.org/10.1021/acs.analchem.8b03043.
[40] V.S. Joshi, J. Kreth, D. Koley, Pt-decorated MWCNTs–ionic liquid composite-based hydrogen peroxide sensor to study microbial metabolism using scanning electrochemical microscopy, Anal. Chem. 89 (2017) 7709–7718, https://doi.org/10.1021/acs.analchem.7b01677.
[41] N.M. Jayathilake, D. Koley, Glucose microsensor with covalently immobilized glucose oxidase for probing bacterial glucose uptake by scanning electrochemical microscopy, Anal. Chem. 92 (2020) 3589–3597, https://doi.org/10.1021/acs.analchem.9b04284.
[42] Y.-T. Lin, A. Preet, Y.-P. Chiu, B.-S. Yip, H.H. Girault, S. Darvishi, et al., Communication—scanning electrochemical microscopy analysis of Interleukin-6 in oral cancer, ECS J. Solid State Sci. Technol. 9 (2020) 115028, https://doi.org/10.1149/2162-8777/abc058.
[43] L. Huang, Z. Li, Y. Lou, F. Cao, D. Zhang, X. Li, Recent advances in scanning electrochemical microscopy for biological applications, Mater 11 (2018) 1389, https://doi.org/10.3390/ma11081389.
[44] S. Darvishi, H. Pick, T.-E. Lin, Y. Zhu, X. Li, P.-C. Ho, et al., Tape-stripping electrochemical detection of melanoma, Anal. Chem. 91 (2019) 12900–12908, https://doi.org/10.1021/acs.analchem.9b02819.
[45] T.E. Lin, A. Bondarenko, A. Lesch, H. Pick, F. Cortés-Salazar, H.H. Girault, Monitoring tyrosinase expression in non-metastatic and metastatic melanoma tissues by scanning electrochemical microscopy, Angew. Chem. Int. Ed. 55 (2016) 3813–3816, https://doi.org/10.1002/anie.201509397.
[46] T.E. Lin, Y.J. Lu, C.L. Sun, H. Pick, J.P. Chen, A. Lesch, et al., Soft electrochemical probes for mapping the distribution of biomarkers and injected nanomaterials in animal and human tissues, Angew. Chem. Int. Ed. 56 (2017) 16498–16502, https://doi.org/10.1002/anie.201709271.
[47] B. Song, L.G. Leff, Influence of magnesium ions on biofilm formation by Pseudomonas fluorescens, Microbiol. Res. 161 (2006) 355–361, https://doi.org/10.1016/j.micres.2006.01.004.
[48] V. Körstgens, H.-C. Flemming, J. Wingender, W. Borchard, Influence of calcium ions on the mechanical properties of a model biofilm of mucoid Pseudomonas aeruginosa, Water Sci. Technol. 43 (2001) 49–57, https://doi.org/10.2166/wst.2001.0338.
[49] B.M. Appenzeller, C. Yanez, F. Jorand, J.-C. Block, Advantage provided by iron for Escherichia coli growth and cultivability in drinking water, Appl. Environ. Microbiol. 71 (2005) 5621–5623, https://doi.org/10.1128/AEM.71.9.5621-5623.2005.
[50] Y. Fan, R. Hao, C. Han, B. Zhang, Counting single redox molecules in a nanoscale electrochemical cell, Anal. Chem. 90 (2018) 13837–13841, https://doi.org/10.1021/acs.analchem.8b04659.
[51] Z. Hu, J. Jin, H.D. Abruña, P.L. Houston, A.G. Hay, W.C. Ghiorse, M.L. Shuler, G. Hidalgo, L.W. Lion, Spatial distributions of copper in microbial biofilms by scanning electrochemical microscopy, Environ. Sci. Technol. 41 (2007) 936–941, https://doi.org/10.1021/es061293k.
[52] K. Welch, Y. Cai, M. Strømme, A method for quantitative determination of biofilm viability, J. Funct. Biomater. 3 (2012) 418–431, https://doi.org/10.3390/jfb3020418.
[53] F. Kracke, I. Vassilev, J.O. Krömer, Microbial electron transport and energy conservation–the foundation for optimizing bioelectrochemical systems, Front. Microbiol. 6 (2015) 575, https://doi.org/10.3389/fmicb.2015.00575.
[54] Y.-F. Wang, S. Tsujimura, S.-S. Cheng, K. Kano, Self-excreted mediator from Escherichia coli K-12 for electron transfer to carbon electrodes, Appl. Microbiol. Biotechnol. 76 (2007) 1439–1446, https://doi.org/10.1007/s00253-007-1114-6.
[55] L. Wang, M.D. Luca, T. Tkhilaishvili, A. Trampuz, M. Gonzalez Moreno, Synergistic activity of fosfomycin, ciprofloxacin and gentamicin against Escherichia coli and Pseudomonas aeruginosa biofilms, Front. Microbiol. 10 (2019) 2522, https://doi.org/10.3389/fmicb.2019.02522.
[56] A.H. Delcour, Outer membrane permeability and antibiotic resistance, Biochim. Biophys. Acta Proteins Proteom 1794 (2009) 808–816, https://doi.org/10.1016/j.bbapap.2008.11.005.
[57] B.U. Tezel, N. Akçelik, F.N. Yüksel, N.T. Karatuğ, M. Akçelik, Effects of sub-MIC antibiotic concentrations on biofilm production of Salmonella infantis, Biotechnol. Biotechnol. Equip. 30 (2016) 1184–1191, https://doi.org/10.1080/13102818.2016.1224981.

Sorour Darvishi received her B.Sc. in Material Science and Engineering from the Isfahan University of Technology (Iran) in 2014. Her undergraduate thesis was based on the effect of thermomechanical processing and grain size of nanocrystalline TiNiCo and TiNi shape memory alloys on corrosion behavior in simulated body fluids. She continued her Master's degree in the same department by working on the development of a non-enzymatic glucose sensor based on Nickel Nanoparticles: Graphene/ Gelatin Methacrylate (GelMa) under the supervision of Prof. Fathallah Karimzadeh and Prof. Mahshid Kharaziha. She finished her graduate studies in 2016 with the honor of the first ranked student in the university in recognition of her excellent academic performance. She started her Ph.D. studies in 2017 at the École Polytechnique fédérale de Lausanne (Switzerland) under the supervision of Prof. Hubert H. Girault and Dr. Andreas Lesch. During her Ph.D. she is working on the electrochemical imaging of tissue and biofilms.

Dr. Horst M. Pick is a senior scientist at the School of Environmental Sciences and Engineering of the Swiss Federal Institute of Technology (EPFL) in Lausanne, Switzerland. He obtained his PhD in Microbiology and Genetics in 1995 from the University of Basel (Biozentrum), Basel, Switzerland. His research focuses on the effects of man-made chemical pollutants on the environment and human health.

Dr. Emad Oveisi is a senior staff scientist at the Interdisciplinary Centre for Electron Microscopy (CIME) at EPFL. He received an MSc in Materials Science and a BSc in Metallurgy and Materials Engineering both from the University of Tehran, Iran. He received in 2014 PhD in Materials Science from EPFL, Switzerland. Since April 2015 he is leading the electron microscopy platform of EPFL-Valais. Emad Oveisi's research focuses on the application and development of electron microscopy techniques, with emphasis on 3D imaging of crystal defects as well as the precision measurement of materials properties using aberration-corrected S/TEM. In 2018, he received the prestigious *Microscopy Today Innovation Award* for inventing "Single-shot three-dimensional electron imaging", a novel technique that enables 3D imaging of *in situ* dynamics.

Dr. Hubert H. Girault is Professor at the Ecole Plotechnique Fédérale de Lausanne and the Director of the Laboratory of Physical and Analytical Chemistry since 1992. His research interest includes electrochemistry of soft interfaces and electrochemical sensors including scanning electrochemical microscopy (SECM), non-linear spectroscopy, mass spectrometry and electrochemical energy storage, *e.g.* redox flow batteries and hydrogenproduction.

Dr. Andreas Lesch is since November 2018 Senior Assistant Professor of Analytical Chemistry at the University of Bologna, Department of Industrial Chemistry "Toso Montanari". He obtained a PhD at the University of Oldenburg, Department of Pure and Applied Chemistry, in Germany in 2012. Thereafter, he worked six years at the Ecole Polytechnique Fédérale de Lausanne (EPFL) in physical and analytical electrochemistry. His current main research interests are in the micro-electroanalytical detection of analytes in biological systems, which includes the development and application of inkjet-printed biosensors and soft probes for scanning electrochemical microscopy.